PUBLIC HEALTH

Genomic epidemiology unveils the dynamics and spatial corridor behind the Yellow Fever virus outbreak in Southern Brazil

Marta Giovanetti[1,2,3]†, Francesco Pinotti[4]†, Camila Zanluca[5]†, Vagner Fonseca[6]†, Taishi Nakase[7], Andrea C. Koishi[5], Marcel Tscha[5], Guilherme Soares[5], Gisiane Gruber Dorl[5], Antônio Ernesto M.L Marques[5], Renato Sousa[8], Talita Emile Ribeiro Adelino[9], Joilson Xavier[2,10], Carla de Oliveira[1,2], Sandro Patroca[11], Natalia Rocha Guimaraes[9], Hegger Fritsch[2,10], Maria Angélica Mares-Guia[1], Flavia Levy[1], Pedro Henrique Passos[12], Vinicius Leme da Silva[13], Luiz Augusto Pereira[13], Ana Flávia Mendonça[13], Isabel Luana de Macêdo[14], Davi Emanuel Ribeiro de Sousa[14], Gabriela Rodrigues de Toledo Costa[15], Marcio Botelho de Castro[14,16], Miguel de Souza Andrade[17], Filipe Vieira Santos de Abreu[18], Fabrício Souza Campos[19], Felipe Campos de Melo Iani[9], Maira Alves Pereira[9], Karina Ribeiro Leite Jardim Cavalcante[12], Andre Ricardo Ribas de Freitas[20], Carlos Frederico Campelo de Albuquerque[6], Eduardo Marques Macário[21], Marlei Pickler Debiasi dos Anjos[22], Rosane Campanher Ramos[23], Aline Alves Scarpellini Campos[24], Adriano Pinter[25], Marcia Chame[26], Livia Abdalla[26], Irina Nastassja Riediger[27], Sérvio Pontes Ribeiro[28], Ana I. Bento[29], Tulio de Oliveira[30], Carla Freitas[31], Noely Fabiana Oliveira de Moura[32], Allison Fabri[1], Cintia Damasceno dos Santos Rodrigues[1], Carolina Cardoso Dos Santos[1], Marco Antonio Barreto de Almeida[24], Edmilson dos Santos[24], Jader Cardoso[24], Douglas Adriano Augusto[33], Eduardo Krempser[33], Luís Filipe Mucci[34,35,36], Renata Rispoli Gatti[37], Sabrina Fernandes Cardoso[37,38], João Augusto Brancher Fuck[39], Maria Goretti David Lopes[40], Ivana Lucia Belmonte[40], Gabriela Mayoral Pedroso da Silva[40], Maiane Regina Ferreira Soares[40], Marilia de Melo Santos de Castilhos[40], Joseana Cardoso de Souza e Silva[40], Alceu Bisetto Junior[40], Emanuelle Gemin Pouzato[40], Laurina Setsuko Tanabe[40], Daniele Akemi Arita[40], Ricardo Matsuo[40], Josiane dos Santos Raymundo[40], Paula Cristina Linder Silva[40], Ana Santana Araújo Ferreira Silva[40], Sandra Samila[40], Glauco Carvalho[9], Rodrigo Stabeli[6], Wildo Navegantes[6], Luciano Andrade Moreira[41], Alvaro Gil A. Ferreira[41], Guilherme Garcia Pinheiro[2], Bruno Tardelli Diniz Nunes[11], Daniele Barbosa de Almeida Medeiros[11], Ana Cecília Ribeiro Cruz[11], Rivaldo Venâncio da Cunha[42], Wes Van Voorhis[43], Ana Maria Bispo de Filippis[1], Maria Almiron[44], Edward C. Holmes[45], Daniel Garkauskas Ramos[12], Alessandro Romano[12], José Lourenço[46]‡*, Luiz Carlos Junior Alcantara[1,2]‡*, Claudia Nunes Duarte dos Santos[5]‡*

Despite the considerable morbidity and mortality of yellow fever virus (YFV) infections in Brazil, our understanding of disease outbreaks is hampered by limited viral genomic data. Here, through a combination of phylogenetic and epidemiological models, we reconstructed the recent transmission history of YFV within different epidemic seasons in Brazil. A suitability index based on the highly domesticated *Aedes aegypti* was able to capture the seasonality of reported human infections. Spatial modeling revealed spatial hotspots with both past reporting and low vaccination coverage, which coincided with many of the largest urban centers in the Southeast. Phylodynamic analysis unraveled the circulation of three distinct lineages and provided proof of the directionality of a known spatial corridor that connects the endemic North with the extra-Amazonian basin. This study illustrates that genomics linked with eco-epidemiology can provide new insights into the landscape of YFV transmission, augmenting traditional approaches to infectious disease surveillance and control.

INTRODUCTION

Yellow fever virus (YFV) is a single-stranded positive-sense RNA virus belonging to the genus *Flavivirus*, family *Flaviviridae* (*1*). This mosquito-borne pathogen is currently endemic in tropical areas of Africa and South America. YFV can be maintained in two transmission cycles: the sylvatic (or jungle) and the urban cycles. The sylvatic cycle involves nonhuman primates (NHPs) and forest canopy-dwelling mosquitoes, mainly *Sabethes* sp. and *Haemagogus* sp. (*2*). While African NHPs seemingly rarely die from YFV infection, New World NHPs typically exhibit disease

signs with elevated mortality rates and thus act as sentinel animals for viral circulation in the environment, in turn representing a valuable marker for epidemiological surveillance (3). Within the urban cycle, YFV is transmitted to humans by highly anthropophilic *Aedes* sp. mosquito vectors (2) that are typically widely distributed in urban settings in South America and Africa.

In Brazil, yellow fever transmission historically occurs within a sylvatic cycle in the Amazonian region (4). In the extra-Amazonian region, yellow fever outbreaks occur with potential infection to humans with irregular periodicity under favorable conditions for transmission, such as a build-up of susceptible hosts, below threshold human vaccine coverage, high vector density, favorable temperature and rainfall, or the emergence of viral strains with potentially increased fitness advantage (5, 6). In recent decades, YFV reemergence events have had a great impact on public health in Brazil (7). In 2002–2003, 2007–2009, and the during the ongoing outbreak (2016–2019 and 2020-present), there has been a spatial expansion of YFV circulation, with the virus spreading from the east toward the south of Brazil, reaching the state of Rio Grande do Sul located at the extreme meridional region of the country (8–10). During these outbreaks, thousands of NHPs deaths were documented, mostly in *Alouatta* sp. (i.e., howler monkeys), followed by *Callithrix* sp. and *Cebus* sp. (10, 11), and in the most recent circulation, the virus was detected in *Leontopithecus* sp., an endemic highly endangered species (3). In addition, more than 2100 human cases were reported in the Southeast region of Brazil, with a case fatality rate of ~30%, many of them in areas with low human vaccination coverage (8, 12).

In September 2020, a novel YFV reemergence was observed within the midwestern states of Goiás, Distrito Federal and the Southeast state of Minas Gerais (13, 14). This reemergence was concomitant with the outbreak that started in 2016 and is ongoing in the Southern region of the country (15), increasing the complexity of the Brazilian epidemiological scenario and the risk to public health (3, 13). While the urban cycle of yellow fever has been absent in Brazil since 1942 (16), these recent outbreaks have occurred in proximity to areas heavily infested by potential *Ae. aegypti* and *Ae. albopictus* vectors that are close to large, densely populated metropolitan regions. These areas are also characterized by low YFV vaccination coverage, thereby representing a risk for the re-establishment of the urban cycle (10). Previous studies have analyzed the spatial and evolutionary dynamics of the current YFV outbreak in different Southeastern states (7) and have documented the cocirculation of distinct YFV lineages (17, 18). Nevertheless, a shortage of genomic data from many locations and time points has hampered the ability to understand in detail the reemergence and establishment of YFV transmission across extra-Amazonian regions (7, 18).

Identifying spatial corridors of YFV spread, their ecological backgrounds, the underlying human immunity landscape, as well as the role of the animal vertebrate hosts and vector populations are crucial to predicting, preventing, and controlling future potential outbreaks events that may lead to epidemics. To gain better insights into the routes of YFV dispersion, we tracked the spread and reemergence of the virus by analyzing metadata on human infections and newly 147 genome sequences sampled mainly from NHPs, as well as from some human patients within the Northern, Midwestern, Southeastern, and Southern regions of Brazil.

[1]Laboratório de Flavivírus, Instituto Oswaldo Cruz, Fundação Oswaldo Cruz, Rio de Janeiro, Brazil. [2]Instituto Rene Rachou, Fundação Oswaldo Cruz, Belo Horizonte, Minas Gerais, Brazil. [3]Department of Science and Technology for Humans and the Environment, Università of Campus Bio-Medico di Roma, Italy. [4]Department of Zoology, University of Oxford, Oxford, OX3 7BN, UK. [5]Laboratório de Virologia Molecular, Instituto Carlos Chagas/Fiocruz-PR, Curitiba, Paraná, Brazil. [6]Organização Pan-Americana da Saúde/Organização Mundial da Saúde, Brasília, Distrito Federal, Brazil. [7]Nuffield Department of Medicine, University of Oxford, Oxford, OX3 7BN, UK. [8]Laboratório de Patologia Veterinária, Hospital Veterinário UFPR, PR Brazil. [9]Laboratório Central de Saúde Pública do Estado de Minas Gerais, Fundação Ezequiel Dias, Belo Horizonte, Minas Gerais, Brazil. [10]Universidade Federal de Minas Gerais, Belo Horizonte, Minas Gerais, Brazil. [11]Evandro Chagas Institute, Para, Brazil. [12]Coordenação Geral das Arboviroses, Secretaria de Vigilância em Saúde/Ministério da Saúde (CGARB/SVS-MS), Brasília, Distrito Federal, Brazil. [13]Laboratório Central de Saúde Pública Dr Giovanni Cysneiros, Goiânia, Goiás, Brazil. [14]Veterinary Pathology Laboratory, Campus Darcy Ribeiro, University of Brasília, Brasília, DF 70636- 200, Brazil. [15]Environmental Health Surveillance, Directorate of the Federal District (DIVAL), DF 70790-060, Brazil. [16]Graduate Program in Animal Sciences, College of Agronomy and Veterinary Medicine, University of Brasília, Brasília, DF 70910-900, Brazil. [17]Baculovirus Laboratory, Department of Cell Biology, Institute of Biological Sciences, University of Brasilia, Brasília 70910-900, DF, Brazil. [18]Insect Behavior Laboratory, Federal Institute of Northern Minas Gerais, Salinas 39560-000, MG, Brazil. [19]Institute of Basic Health Sciences, Federal University of Rio Grande do Sul, Porto Alegre 90035-003, RS, Brazil. [20]Faculdade de Medicina São Leopoldo Mandic, Campinas, SP, Brazil. [21]Superintendência de Vigilância em Saúde – SES – Santa Catarina, South Brazil. [22]Laboratorio central de Saude Publica de Santa Catarina, Superintendência de Vigilância em Saúde – SES – Santa Catarina, South Brazil. [23]Laboratório Central de Saúde Pública do Estado do Rio Grande do Sul, Superintendência de Vigilância em Saúde – SES – Santa Catarina, South Brazil. [24]Secretaria Estadual de Saúde do Rio Grande do Sul, Centro Estadual de Vigilância em Saúde, Porto Alegre, RS, Brazil. [25]Departamento de Medicina Veterinária Preventiva e Saúde Animal, Faculdade de Medicina Veterinária e Zootecnia, Universidade de São Paulo, São Paulo, 05508-000, Brazil. [26]Oswaldo Cruz Foundation, Biodiversity, Wildlife Health Institutional Platform (PIBSS/Fiocruz), Rio de Janeiro, Brazil. [27]Laboratório Central de Saúde Pública do Estado do Paraná (Lacen-PR), Curitiba, Paraná, Brazil. [28]Laboratory of Ecology of Diseases & Forests, NUPEB/ICEB, Federal University of Ouro Preto, Minas Gerais, Brazil. [29]Pandemic Prevention Initiative, The Rockefeller Foundation, Washington DC, USA. [30]School for Data Science and Computational Thinking, Faculty of Science and Faculty of Medicine and Health Sciences, Stellenbosch University, South Africa. [31]Secretaria de Vigilância em Saúde, SVS, Brazilian Ministry of Health, Brasilia, Federal District, Brazil. [32]Oswaldo Cruz Foundation, Fiocruz, Brasilia, Federal District, Brazil. [33]Plataforma Institucional Biodiversidade e Saúde Silvestre - Centro de Informação em Saúde Silvestre (CISS) - Fiocruz/RJ, Avenida Brasil, 4365. Manguinhos - Rio de Janeiro - RJ Cep: 21.040-360. [34]Secretaria da Saúde (São Paulo - Estado), Av Dr. Enéas Carvalho de Aguiar, 188 - Cerqueira César, São Paulo - SP, 05403-000, Brazil. [35]Coordenadoria de Controle de Doenças (CCD), Av. Dr. Enéas Carvalho de Aguiar, 188 - Cerqueira César, São Paulo - SP, 05403-000, Brazil. [36]Instituto Pasteur (IP), Av. Paulista, 363 Cerqueira Cesar – São Paulo- SP – CEP:01311-000. [37]Secretaria de Estado da Saude de Santa Catarina, R. Esteves Júnior, 160 - Centro, Florianópolis - SC, 88015-130, Brazil. [38]Department of Cell Biology, Embryology and Genetics, Federal University of Santa Catarina (UFSC), Florianópolis, Brazil. [39]Diretoria de Vigilância Epidemiológica da Secretaria de Estado da Saúde de Santa Catarina, R. Esteves Júnior, 160 - Centro, Florianópolis - SC, 88015-130, Brazil. [40]Secretaria de Estado da Saúde do Paraná, Brazil, R. Piquiri, 170 - Rebouças, Curitiba - PR, 80230-140. [41]Mosquitos Vetores: Endossimbiontes e Interação Patógeno-Vetor, Instituto René Rachou–Fiocruz, Belo Horizonte 30190-002, MG, Brazil. [42]Fundação Oswaldo Cruz, Bio-Manguinhos, Rio de Janeiro, Rio de Janeiro, Brazil. [43]Center for Emerging and Re-emerging Infectious Diseases (CERID), University of Washington, Seattle, WA, USA. [44]Pan American Health Organization/World Health Organization, Washington, DC, USA. [45]Marie Bashir Institute for Infectious Diseases and Biosecurity, School of Life and Environmental Sciences and School of Medical Sciences, University of Sydney, Sydney, NSW, Australia. [46]BioISI (Biosystems and Integrative Sciences Institute), Faculdade de Ciências da Universidade de Lisboa, Campo Grande, 1749-016 Lisboa Portugal.

*Corresponding author. Email: claudia.dossantos@fiocruz.br (C.N.D.d.S.); luiz.alcantara@ioc.fiocruz.br (L.C.J.A.); jmlourenco@fc.ul.pt (J.L.)

†These authors contributed equally to this work.
‡These authors contributed equally to this work.

RESULTS

Human incidence of YFV in Brazil

Because of inherent natural variations in mosquito population size, YFV should display temporal dynamics with an oscillatory behavior characterized by recurrent peak incidence every epidemic season (local mid-summer) (19). However, limited surveillance and local testing capacity mean that obtaining a detailed spatio-temporal perspective with high resolution, and within Brazilian microregions, is challenging. Nonetheless, the epidemic curves of human case reports in the study period showed clear seasonal outbreaks within several national macroregions, compatible with the periods previously detected and used for national surveillance (Fig. 1A) (20). In particular, between 2015 and 2022, there were three outbreaks in the Southeast (2016–2019), followed by two smaller outbreaks in the South (2020–2021).

We estimated transmission potential of a specific virus by a specific mosquito species (21, 22). Because of lack of data related to mosquito species that drive YFV transmission within the animal reservoir, we were restricted to calibrating the index specifically to *Aedes aegypti* and have thus interpreted the suitability measure as a proxy for spillover risk into human populations rather than a measure of transmission potential overall (see Materials and Methods and Supplementary Text for full details). The index *P* based on local climatic variables averaged across the macroregions presented clear seasonal oscillations matching the time windows of the observed waves of infection in humans (Fig. 1A). The majority of human reported infections also took place in inter-yearly periods that had higher index *P* values (Fig. 1A, inner plot). When looking at the years 2017–2019 for which incidence presented a clearer seasonal signal, we found a positive correlation between cases and index *P* of 0.47 (*P* value = 0.003). As shown in previous studies, index *P* often precedes incidence in time due to inherent natural lags between natural climate variation and its effects on transmission (22) or due to delays in reporting. Accordingly, we found that an optimal shift of index *P* by +1 month into the future maximized the correlation with incidence at 0.73 (*P* value = 5.7×10^{-07}).
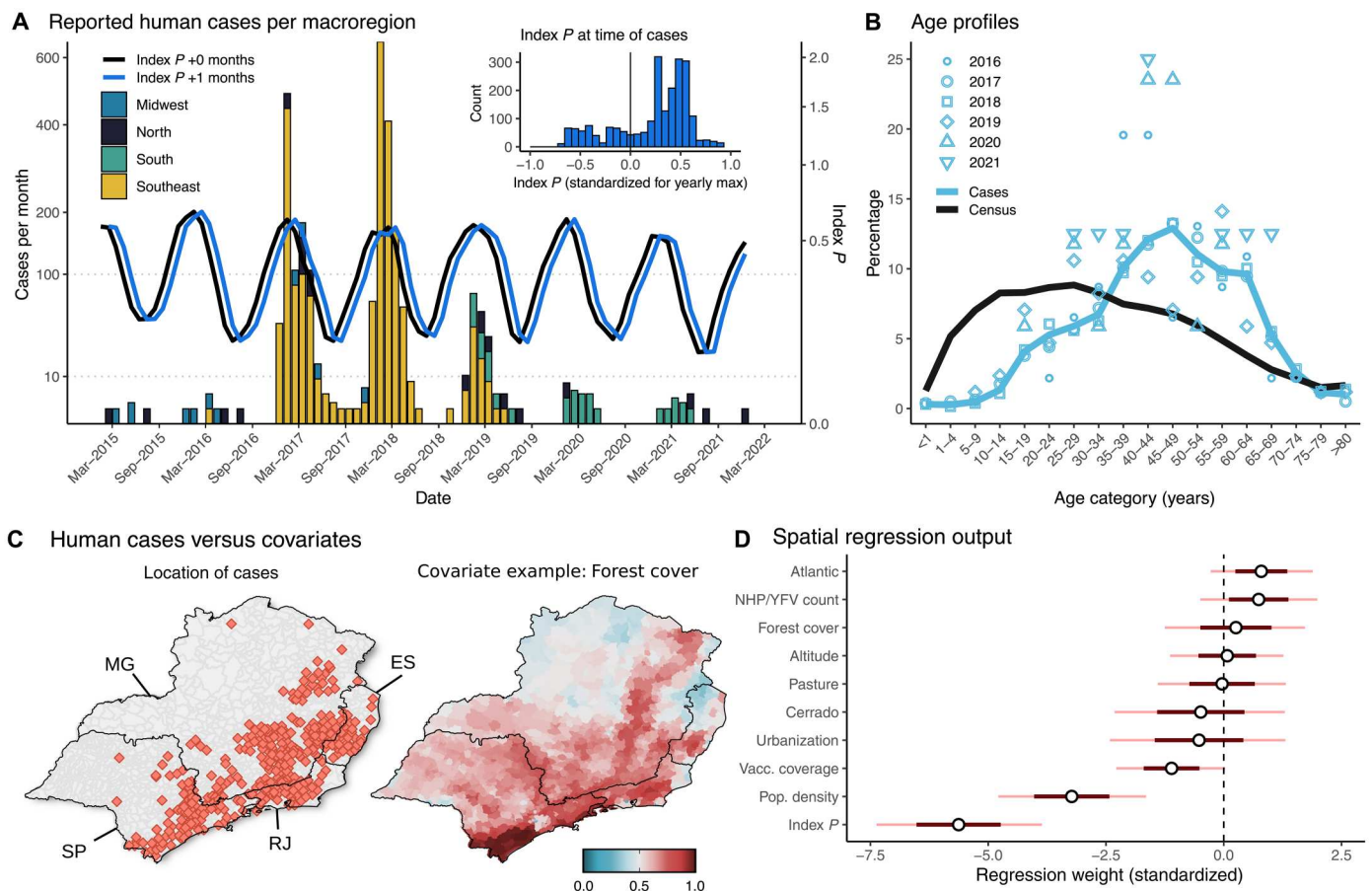
Fig. 1. Human incidence of YFV in Brazilian macroregions, 2015–2022. (**A**) Time series of monthly reported human cases in four Brazilian macroregions (those reporting the majority of cases) and monthly mosquito-viral suitability measure (index *P*) aggregated (mean) across the macroregions. Index *P* is calibrated to YFV and *Aedes aegypti*, interpreted as spillover risk, and presented here index *P* is presented by the lines as baseline (black) and shifted by +1 month (blue). The inset plot shows the distribution (*y* axis) of human cases according to the value of index *P* (*x* axis) extracted at each time point of reported human YFV cases (shifted +1 month, standardized by yearly maximum). (**B**) Age distribution of human cases across the years (light blue) versus Census 2010 data (black), both aggregated across the Southeast and South macroregions. (**C**) Spatial distribution of human cases (red filled points) and one example of a spatial covariate (forest cover) used for modeling the Southeast macroregion. For all covariates, see fig. S1. Covariates were normalized by their maximum for visualization, with covariates population density, Atlantic and NHP cases first transformed with $\log_{10}$ (color scale in the bottom right). Spatial boundaries (black) are states: São Paulo (SP), Espírito Santo (ES), Minas Gerais (MG), Rio de Janeiro (RJ). (**D**) Marginal posterior distributions (standardized to appear on the same scale) for individual regression weights for the 10 covariates explored.

Hence, the index was able to capture the time-varying spillover risk of YFV from the animal reservoir, suggesting that local climate variation and its effects on mosquito populations, specifically *A. aegypti*, may dictate the timing of observed spillover events.

In accordance with previous studies [(e.g., *23*)], we found that incidence across the entire time and spatial ranges of observation were characterized by an older age profile compared to that of the population within the macroregions (Fig. 1B). Overall, the highest burden was found in the 45 to 49 age group (~13% of cases) which was at odds with a much younger age profile of the local population. Also, in agreement with previous studies (*7, 23*), incidence was higher among males (~82% of all cases), in a background of ~49% of the population being male within those macroregions.

We explored the spatio-temporal association between human case counts with 10 covariates at the municipality level (figs. S1 and S2), including the index *P* (proxy for spillover risk), human population density, vaccination coverage, Cerrado and Atlantic Forest biomes, pasture and urbanization land uses, forest cover and NHP YFV counts (tables S2 and S3). We focused on the states of São Paulo, Minas Gerais, Espírito Santo, and Rio de Janeiro, which together reported 2210 of the 2289 human cases (97%) in our dataset (Fig. 1C). To quantify the roles of each covariate, we applied a Bayesian spatial regression model at the municipality level (Supplementary Text). Our analysis revealed considerable overdispersion due to unobserved random spatial effects (fig. S3), such that the 10 covariates could not explain the spatial distribution of reported human cases alone. Although not possible to demonstrate with available data, we note that one possible contributing factor for such unobserved random spatial effects could have been differences in reporting effort across the municipalities. The estimated posterior distributions for the regression coefficients of each covariate (Fig. 1D and table S4) showed results compatible with expectations from the visual inspection of spatial distributions, with four variables having positive effects and six having negative effects (Fig. 1D and fig. S3). Notably, there was a positive association of human cases with the Atlantic Forest biome and occurrence of NHP/YFV cases and negative associations with vaccination coverage, population density, and index *P* (Fig. 1D). The index *P* had the strongest negative effect, which contrasted the positive time-based correlation of human cases with the index (Fig. 1A). While this may be counterintuitive at first, we note that the index *P* was calibrated specifically to *A. aegypti* due to lack of data for calibration to mosquito species driving transmission in the animal reservoir. The index is here interpreted as a measure of spillover risk by *A. aegypti*, and its negative spatial relationship with reported cases simply reveals that the municipalities with most spillover events are not necessarily the ones with highest suitability for transmission with *A. aegypti*. This is also revealed by the strong negative association of the index *P* with other local factors positively associated with reported YFV cases, such as forest biome type, forest cover, and altitude (fig. S4). This mix of covariate contributions reinforced the notion that reported human cases typically result from transmission events associated with regions reporting NHP cases within or bordering forested environments, with lower vaccine coverage and human population density (*24, 25*), which are not necessarily regions with the most favorable conditions for transmission by *Aedes aegyti*.

We further mapped the predicted probability of human YFV case reporting (from the spatial regression model) and the covariate of vaccine coverage (Fig. 2, A and B). When these variables were superimposed into a bivariate map, spatial hotspots emerged with both high probability of reporting and proportion unvaccinated toward the southeast of the study area (Fig. 2C). While recent past reporting was negatively associated with human population density (Fig. 1D), many of the largest cities in the area of study were found to be peripheral to these hotspots, highlighting areas with large human populations susceptible to future outbreaks events (Fig. 2C). This was particularly the case for the states of São Paulo (cities of São Paulo, Campinas, and Guarulhos), Minas Gerais (Belo Horizonte and Contagem), and Espiríto Santo (Serra, Vila Velha, and Cariacica). For the state of Rio de Janeiro, the largest cities were characterized by a mix of a high proportion of unvaccinated individuals and an intermediate probability of reporting but were closely surrounded by hotspots of low vaccination coverage and high levels of reporting to the north. The only large city seemingly not closely connected to such a hotspot was Uberlândia (Minas Gerais), which had intermediate vaccination levels and low risk of occurrence. The identification of these hotspots, characterized by a mix of historical case reporting and a proportion of unvaccinated individuals living in close proximity to the largest cities, highlights areas of critical importance in which vaccination coverage and surveillance need to be enhanced in the near future.

Phylodynamics of YFV in Brazil

To explore the phylodynamics of YFV in Brazil, we combined our 147 newly generated sequences obtained from the Southeastern, Midwestern, and Southern macroregions of the country to those of other genomes available on GenBank (*n* = 296), belonging to the South American I genotype (dataset 1, see Materials and Methods for more details). Our analysis revealed the circulation of three different clades, named hereafter as clades Ia, IIb, as well as a novel clade termed IIIc (Fig. 3). Through analysis of the genomic dataset that included samples collected in 2017 from the North macroregion, we were able to identify a corridor of viral spread associated with clade IIIc [Fig. 3; posterior probability (pp), 1.0] that connected the endemic North with the extra-Amazonian basin (states of Goiás and Distrito Federal in the Midwest and the state of Minas Gerais in the Southeast). We estimated the mean time of the most recent common ancestor (tMRCA) for this clade to be July 2016 [95% highest posterior density (HPD) interval, April 2015–March 2017]. In addition, we found that circulating clades Ia to IIIc were characterized by specific mutational signatures, including nonsynonymous changes in the RNA-dependent RNA polymerase (RdRp): S8053D and T9806I in clade Ia, V8048I in clade IIb, and G8048A in clade IIIc. These four nonsynonymous and other six synonymous mutations are described in table S5.

To investigate the evolution of clades Ia and IIb in more detail, we used smaller datasets derived from each clade individually (dataset 2 and dataset 3 respectively, see Materials and Methods for more details). Before phylogeographic analysis, each clade was also assessed for molecular clock signal using the root-to-tip regression method available in TempEst v1.5.3 (*26*), following the removal of potential outliers that may strongly violate the assumption of rate constancy. The final dataset included *n* = 163 genome sequences for clade Ia and *n* = 270 genome sequences for clade IIb. There was a strong correlation between sampling time and the root-to-tip divergence in the two datasets (Fig. 4A and 5A), indicative of a constancy of evolutionary rate and hence allowing the use of molecular clock
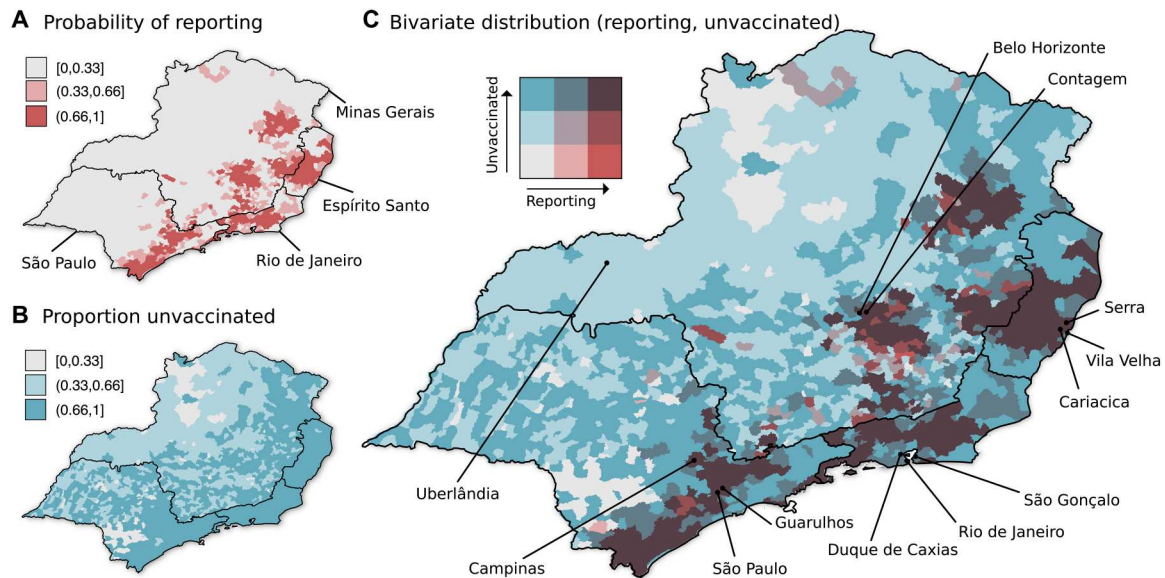
Fig. 2. Spatial hotspots as a mixture of past reporting and proportion unvaccinated. (**A**) Probability of reporting of human YFV cases per municipality as predicted by the spatial regression model. (**B**) Proportion unvaccinated (1, vaccination coverage) per municipality. (A and B) Variables are discretized into three categories to provide a bivariate color scale in (C) with a maximum of nine colors for best interpretability. (**C**) Spatial distribution of both probability of occurrence and proportion unvaccinated presented in bivariate color scale. Spatial distribution of both probability of occurrence and proportion unvaccinated presented in bivariate color scale [i.e., (A) and (B) superimposed into a bivariate color scale]. The three largest cities in each state are highlighted (São Paulo: São Paulo, Guarulhos, Campinas; Minas Gerais: Belo Horizonte, Uberlândia, Contagem; Rio de Janeiro: Duque de Caxias, Rio de Janeiro, São Gonçalo; Espírito Santo: Serra, Vila Velha, Cariacica).

models to infer evolutionary parameters. Our phylogeographic reconstruction of clade Ia (Fig. 4B) suggested a mean time of origin in late-July 2015 [95% highest posterior density (HPD): 29 March 2015 to 18 August 2015]. Viruses from this clade spread from the Northern region of the state of Minas Gerais toward the Southeast and later to the Northeast, as indicated by isolates from the Bahia state.

A different spatial pattern was observed for clade IIb (Fig. 5) compared to clade Ia (Fig. 4). Specifically, clade IIb originated with a mean date in late November 2015 [95% highest posterior density (HPD): 28 November 2015 to 05 January 2016] with an early dispersal from the Midwest (state of Goiás) to the Southeast (Minas Gerais, Espírito Santo, and São Paulo) and later to the South (state of Paraná, Santa Catarina, and Rio Grande do Sul) where it persisted at least until the end of 2021 (Fig. 5B).

Through analysis of the genomic dataset that included samples collected in 2017 from the North macroregion, we were able to identify a corridor of viral spread associated with clade IIIc (Fig. 3; pp, 1.0) that connected the endemic North with the extra-Amazonian basin (states of Goiás and Distrito Federal in the Midwest and the state of Minas Gerais in the Southeast). We estimated the mean tMRCA for this clade to be July 2016 [95% highest posterior density interval (HPD), April 2015–March 2017].

DISCUSSION

The circulation of YFV has been reported in the extra-Amazonian regions of Brazil since the early 2000s (8–10, 27, 28). During this period, many advances have been achieved in the country regarding surveillance in both the reservoir and human population, such as the start of many digital platforms for animal and case reporting (e.g., https://sissgeo.lncc.br/). Preliminary studies demonstrated that a later reemergence, which began in 2016, resulted in widespread virus dissemination and an extended period of transmission still active in 2022 (15, 29). The uninterrupted circulation of YFV in the extra-Amazonian environment for a period that exceeds 7 years is unprecedented and coincides with ongoing ecological changes. For example, increases in temperature and precipitation in some areas of the Atlantic Forest biome in the South and Southeast may be contributing to creating conditions for the maintenance of perennial foci of YFV transmission in or around highly populated areas (30, 31). At the same time, while it remains difficult to quantify direct causal effects of landscape changes due to human intervention, the midwestern and southeastern states analyzed in this study are known to be experiencing rapid alterations. Changes in the forestry legislation that took effect in 2016 have allowed and fomented degradation of forested environments; for example, decreasing the size of protected forests along rivers that are expected to increase exposure of adult, male, and poor rural workers involved in logging and farming (32, 33). By 2017, a record primary forest deforestation was measured along the Doce river valley in the state of Minas Gerais (34). Coinciding with this, as reported by Rosser and colleagues (35), the reemergence of YFV in the state of Minas Gerais was observed during a severe drought period. This may have contributed to the spread of YFV at rural-urban boundaries, creating environmental pressures that sparked its reemergence close to Brazil's southeastern cities. In parallel, the number of forest fires in the region where YFV reemerged in 2020 more than doubled in 2018 and 2019 (36). Such landscape changes are driven by the need to de-forest environments for agricultural purposes on a large scale, and 2020 may represent a year of greater exposure of workers to degraded forests and secondary forests (37, 38). This recent trend is unlikely to change drastically in coming years, and the exploration of the role of degraded forested
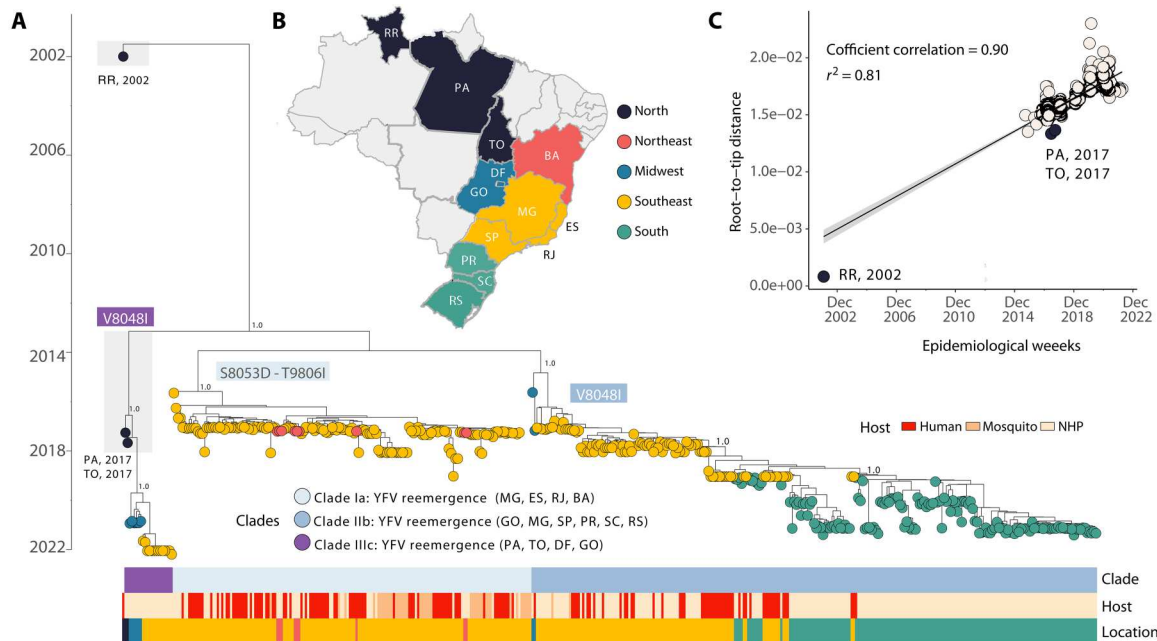
Fig. 3. YFV South America I genotype in Brazil. (**A**) MCC phylogeny inferred using the 147 novel sequences obtained in this study plus 296 publicly available sequences from GenBank. Colors represent different sampling locations (Brazilian states). Colored bars below the tree represent the (top) clade (middle) host and Brazilian macroregion of sampling. Clade-defining mutations have been highlighted on each branch. (**B**) Map of Brazil presenting the states under investigation highlighted within macroregions: RR, Roraima; PA, Pará; DF, Distrito Federal; GO, Goiás; BA, Bahia; MG, Minas Gerais; ES, Espírito Santo; RJ, Rio de Janeiro; SP, São Paulo state; PR, Paraná; SC, Santa Catarina; RS, Rio Grande do Sul. (**C**) Root-to-tip regression of sequence sampling date against genetic divergence from the root of the outbreak clade. Sequences from the endemic Amazon basin (states of Roraima, Pará, and Tocantins) are highlighted.

environments in increased risk of YFV spillover from the NHP hosts should be the focus of future research.

In recent years, thousands of cases and deaths, mainly among NHPs, have caused unprecedented impacts on these animal populations and public health, resulting in raised awareness and control activities, such as the increase of vaccine coverage to classically nonendemic territories (*15, 29*). These recent trends also relate to conservation efforts for NHPs. For example, in the context of the endangered *Alouatta guariba clamitans*, previous work suggests that YFV infection is a major threat for population stability, since outbreaks in fragmented, metapopulation-structured populations are likely to result in local extinctions (*11, 39*). In parallel, an ongoing decline in the size of the Atlantic Forest protected areas, due to recent government policies and the abandonment of surveillance and law enforcement, might have both increased the risks of new NHP outbreaks and, consequently, chances the infection to humans in the environs of areas with high population density.

Previous studies have examined the spatial and evolutionary dynamics of YFV between 2016 and 2019 (*7, 18*). Unfortunately, however, the shortage of genomic data has hampered our ability to understand particular aspects of this epidemic, such as the current reemergence in the Southeast (since late 2019). In this study, we presented a combination of epidemiological and genomic analysis of novel YFV data with the aim of further understanding and describing the past and present of the ongoing epidemic.

A time series of reported human cases between 2015 and 2022 showed a typical yearly seasonal pattern associated with a midsummer peak in January, as well as three outbreaks in the Southeast

(2017–2019) followed by two outbreaks in the South (2020–2021). In general, reporting was associated with areas peripheral or within forested environments characterized by an Atlantic Forest biome, to males and older age groups, to variation in climate, population density, and vaccination coverage. The suitability index used was calibrated to the urban cycle vector *A. aegypti* due to lack of data for mosquito vectors of the enzootic transmission cycle. The index was thus interpreted as a proxy for spillover risk and was found to be associated positively with the timing of reported human infections, providing opportunities to estimate time windows of importance for spillover events and surveillance across the country in future studies.

We were able to identify spatial hotspots characterized by both the reporting of human cases and low vaccination coverage, which were critically peripheral to some of the largest human populations in the Southeast. These hotspots demonstrate the recent reporting of cases close to (but not necessarily within) large cities with large susceptible human populations and where *A. aegypti* is also typically abundant, thereby presenting possible ecological boundaries across which urban transmission cycles could become established. A lack of access to detailed reporting of human cases in other regions of Brazil hampered the application of our spatial regression model to a wider spatial scale. However, it remains plausible that similar hotspots exist within other states, including the state of Bahia that served as a corridor for clade Ia into the southern states, is known to be rich in NHP biodiversity, and also harbors large human populations. These hotspots in the Southeast should become the focus of future targeted mosquito and NHP surveillance, as well as public health campaigns to boost public awareness
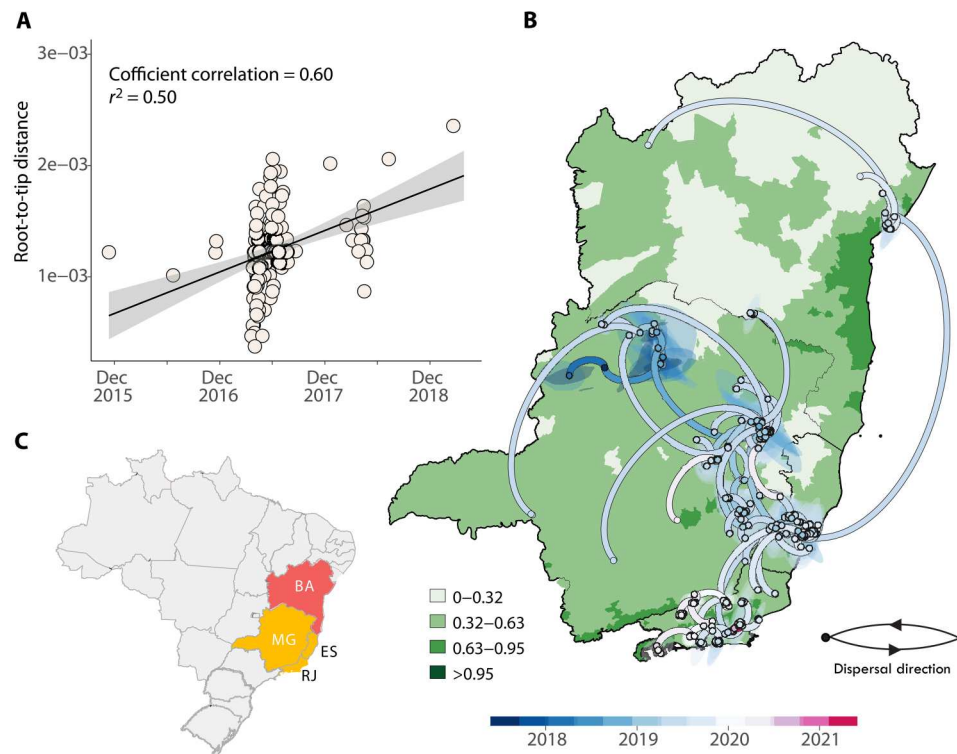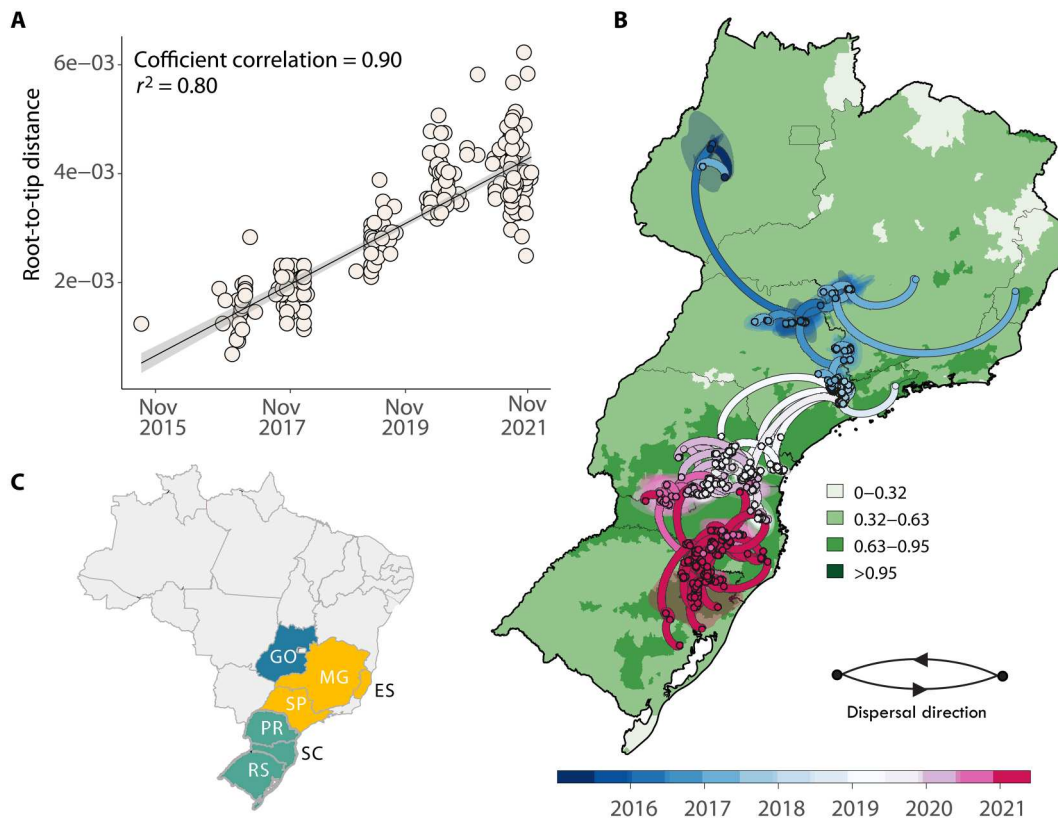
Fig. 4. Spatiotemporal spread of South America I genotype Clade Ia in Brazil. (**A**) Root-to-tip regression of sequence sampling date against genetic divergence from the root of the outbreak clade. (**B**) Phylogeographic reconstruction of the spread of the South America I genotype clade Ia in Brazil (*n* = 163). Circles represent nodes of the MCC phylogeny and are colored according to their inferred time of occurrence. Shaded areas represent the 80% highest posterior density interval and depict the uncertainty of the phylogeographic estimates for each node. Solid curved lines denote the links between nodes and the directionality of movement. Differences in forest coverage population density are shown on a green-white scale. (**C**) Map of Brazil highlighting the spatial area under investigation. MG, Minas Gerais state; ES, Espírito Santo state; RJ, Rio de Janeiro state; BA, Bahia state.

and vaccination coverage in particular within the peripheries of large urban centers. These results are also consistent with the findings of Thoisy *et al.* (*40*), who used ecological niche modeling to demonstrate that the YFV reemergence was associated with biotic factors such as mammal richness, abiotic factors such as temperature and precipitation, and some human-related variables including population density, human footprint, and human vaccination coverage.

Our newly generated YFV sequences were classified to the South American I genotype and formed three distinct clades Ia to IIIc. These clades presented different spatial patterns. Clade Ia historically spread from the Northern region of the state of Minas Gerais toward the Southeast and later to the Northeast. In contrast clade IIb showed an early dispersal from the Midwest (state of Goiás) to the Southeast (Minas Gerais, Espírito Santo, and São Paulo) with a later spread to the South (state of Paraná, Santa Catarina, and Rio Grande do Sul) where it has persisted at least until the end of 2021. While the general spatial spread of clade Ia and IIb have already been described in the Brazilian context (*17, 18*), the analysis of the novel isolates from three macro regions in 2020 and 2021 is novel (North, Midwest, and Southeast). This also allowed us to produce the first genetic evidence in support of a corridor of spread [previously described using NHP case count data (*16*)] associated with clade IIIc which connected the endemic North with the extra-Amazonian basin (states of Goiás, Distrito Federal in the

Midwest, and the state of Minas Gerais in the Southeast). We have identified several point mutations in clades I to III viral genomes, including six associated with amino acid substitutions in nonstructural genes and four with nonsynonymous changes in the RdRp gene. Specifically, clade Ia had two nonsynonymous mutations, S8053D and T9806I, in the RdRp gene; clade IIb had one nonsynonymous mutation, V8048I, in the RdRp gene; and clade IIIc had one nonsynonymous mutation, S8048N, in the RdRp gene. As the RdRp gene is responsible for replicating the viral genome, it is important to further investigate the impact of these mutations on its structure, function, and viral pathogenesis and fitness. In addition, it is worth noting that both nonsynonymous and synonymous mutations in nonstructural genes can cause changes in viral RNA, leading to effects on splicing, stability, translation, or cotranslational protein folding. Therefore, our study emphasizes the need for further research to fully understand the potential impact of these mutations on viral replication.

We failed to identify whether the locations within this corridor (that cuts through the center of the country) had ecological or landscape features of relevance. For example, the associated central regions of Brazil are rich in the Cerrado biome (*41*), which was negatively associated with human YFV case reporting case reporting in our spatial modeling analyses. Compared to elsewhere, these regions are also not particularly suitable for the *Haemagogus and Sabethes* spp. vector species that are associated with the sylvatic

Fig. 5. Spatiotemporal spread of South America I genotype Clade IIb in Brazil. (**A**) Root-to-tip regression of sequence sampling date against genetic divergence from the root of the outbreak clade. (**B**) Phylogeographic reconstruction of the spread of South America I genotype clade IIb in Brazil (*n* = 270). Circles represent nodes of the MCC phylogeny and are colored according to their inferred time of occurrence. Shaded areas represent the 80% highest posterior density interval and depict the uncertainty of the phylogeographic estimates for each node. Solid curved lines denote the links between nodes and the directionality of movement. Differences in forest coverage population density are shown on a green-white scale. (**C**) Map of Brazil highlighting the spatial area under investigation. GO, Goiás state; MG, Minas Gerais state; ES, Espírito Santo state; RJ, Rio de Janeiro state; SP, São Paulo state; PR, Paraná state; SC, Santa Catarina state; RS, Rio Grande do Sul state.

cycle (*42*), nor do they present particular richness of relevant NHP species (*43*). A potential contributing factor could be the large rivers that stem in a north-south axis over the corridor (e.g., Rio Tocantins, Rio das Mortes, and Rio Araguaia), from the state of Pará crossing Tocantins (North) into Goiás (Midwest), the latter at the north border of Minas Gerais (Southeast) as well as the forests on the edges of the north-south oriented mountains that make up the brazilian central plateau. Rivers, mountains, and their associated forest environments offer ideal corridors for NHP settlement and migration, potentially contributing to the spatial spread of YFV (*44*). In this study, we present the first evidence of the north-south directionality of spread over this spatial corridor, which appears particularly related to degraded and deforested riparian forests, raising awareness to its public health importance and suggesting that future research and surveillance initiatives should focus on the associated regions.

It is of relevance to note that our spatial modeling analyses and thus our ability to unravel covariates and drivers of YFV emergence were conditioned by factors related to existing data and its available resolutions. Namely, that various data sources were already aggregated at the municipality level (e.g., vaccination coverage), implying a mismatch of spatial resolution between the explored covariates and a large proportion of the reported YFV infections for which

we had more refined geo-localizations. This meant that while we were able to capture the relationships of covariates with YFV infections across the different municipalities, we were unable to explore the possible role of within-municipality covariate variation. Intuitive examples left unexplored are the covariates of vaccine coverage and forest cover, which are likely to vary substantially within municipality. For example, we were unable to explore the possible relationship between the exact location of forest boundaries and the location of reported YFV cases within each municipality, following the expectation that such ecological boundaries are points of high spillover risk. Similarly, while we recover the expected negative relationship between vaccine coverage and reported YFV cases across municipalities, we were unable to do so between human settlements within a municipality, which may vary significantly in terms of vaccine coverage. Both of these missed opportunities remain as lines of important future research.

Our results reinforce the importance of the North of Brazil as a potential hotspot and revealed a new role for the Midwest regions of the country, in line with studies that have highlighted both regions as relevant hubs, not only for YFV but also for dengue virus (*7, 18, 45*). There were critical gaps in existing genomic data (445 genomes since 2002 with patchy temporal and spatial sampling; fig. S5) which curtailed definite conclusions in this study on key points of the

recent history of YFV in Brazil. There remains, for instance, only a small number of viral genomes from the North, which is a key region for understanding YFV persistence dynamics and genetic diversity. At the same time, although the virus continuously expands its geographical range, there has been historically weak sampling in some states such as Goiás, Distrito Federal, and Minas Gerais that hampered the unraveling of the corridor of spread revealed in the current study.

By identifying spatial corridors of spread, their eco-epidemiological backgrounds, and drivers and mutational signatures associated with successful viral lineages, the combination of epidemiological and genomic surveillance within a One Health approach can have significant public health impact. It can identify the likely places, timings, and processes for the reemergence of urban cycles of transmission, inform on emerging viral lineages that should be the focus of empirical laboratory experimentation, and critically identify areas and time windows where catch-up vaccination campaigns and surveillance initiatives should be directed. Given the existing large gaps in knowledge, there is clearly a need for continued funding for genomic surveillance of YFV both in Brazil and globally.

MATERIALS AND METHODS

Sample collection
Human and NHP samples were collected by local and regional public health authorities, under the guidelines of a national strategy of yellow fever surveillance and sent for molecular diagnostics to the Reference Laboratory of Emerging Viruses of the Carlos Chagas Institute/Fiocruz-PR, which is a Brazilian Ministry of Health Regional Reference Laboratory for arboviruses.

Ethical statement
The project was supported by the Pan American World Health Organization and the Brazilian Ministry of Health as part of the arboviral genomic surveillance efforts within the terms of Resolution 510/2016 of CONEP (Comissão Nacional de Ética em Pesquisa, Ministério da Saúde; National Ethical Committee for Research, Ministry of Health).

Molecular screening and nanopore sequencing
RNA was extracted from tissue samples using the QIAamp Viral RNA Mini KitTM (Qiagen, Hilden, Germany) or the MagMAX pathogen RNA/DNA kit (Life Technologies, Carlsbad, USA) according to the manufacturer's instructions. YFV RNA was detected using the reverse transcription quantitative polymerase chain reaction (RT-qPCR) protocol described by Domingo et al. (46).

cDNA synthesis and whole-genome nanopore sequencing
Sequencing was attempted on 147 selected RT-PCR–positive samples (from a total of 200) regardless of CT value (as previously described) and the availability of epidemiological data (7, 18). All positive samples were submitted to a cDNA synthesis protocol (7) using a ProtoScript II first strand cDNA synthesis kit. A multiplex tiling PCR was then performed using the previously published YFV primer scheme and 30 cycles of PCR using Q5 high-fidelity DNA polymerase (New England Biolabs) as previously described (47). Amplicons were purified using AMPure XP beads (Beckman Coulter), and cleaned-up PCR product concentrations were measured using a Qubit double-stranded DNA (dsDNA) high-sensitivity assay kit on a Qubit 3.0 fluorometer (Thermo Fisher Scientific). DNA library preparation was performed using the Ligation sequencing kit (Oxford Nanopore Technologies) and the Native barcoding kit (NBD103; Oxford Nanopore Technologies, Oxford, UK). A sequencing library was generated from the barcoded products using the genomic DNA sequencing kit SQK-MAP007/SQK-LSK208 (Oxford Nanopore Technologies). The sequencing library was loaded onto a R9.4 flow cell (Oxford Nanopore Technologies). Sample data, location, hosts, NHP species, municipality of collection, and collection date are summarized in Table 1 in the sequencing library.

Generation of consensus sequences
Raw files were basecalled using Guppy v4.5.4, and barcode demultiplexing was performed using qcat. Consensus sequences were generated by de novo assembling using Genome Detective (https://genomedetective.com/) (48). Briefly, Genome Detective uses DIAMOND to identify and classify candidate viral reads in broad taxonomic units, using the viral subset of the Swissprot UniRef90 protein database. Candidate reads are next assigned to candidate reference sequences using National Center for Biotechnology Information (NCBI) blastn and aligned using AGA (Annotated Genome Aligner) and MAFFT. Final contigs and consensus sequences are made available as FASTA files. More detail about Genome Detective can be found in (48).

Collation of YFV complete genome datasets
Genotyping was first conducted using the yellow fever typing tool available at https://genomedetective.com/app/typingtool/yellowfever/ and confirmed using a maximum likelihood (ML) phylogenetic analysis incorporating a collection of representative sequences (n = 495) belonging to the four YFV lineages (fig. S6). This analysis robustly placed the novel YFV sequences generated here into a clade that likely emerged in the state of Roraima in North Brazil in 2002 (fig. S6).

The genome sequences generated here were combined with a dataset comprising previously published genomes from the 2002, 2016 to 2019 YFV epidemics in Brazil (7, 17, 18). Three complete or near complete YFV genome datasets were generated. Dataset 1 (n = 443) comprised the data reported in this study (n = 147) plus (n = 296) complete or near complete YFV genomic sequences (10,000 bp) retrieved from NCBI in September 2022 and covering all the YFV South American (SA) I genotype genomes currently available. This first dataset was used to perform a preliminary comprehensive phylodynamic reconstruction. Subsequently, to understand the transmission and the spatiotemporal evolution of the SA1 lineages 1 and 2 of YFV, genetic analyses were conducted on smaller datasets (dataset 2 and dataset 3, respectively) that included all available genomic sequences belonging to each of those lineages: n = 163 and n = 270, respectively. Dataset 2 was used to reconstruct viral movements across different Brazilian regions (Northeastern, Southeastern, and Midwestern) of clade Ia, while dataset 3 was used to reconstruct viral movements across different Brazilian regions (Midwestern, Southeastern, and Southern) of clade IIb. Sequence alignment was performed using MAFFT (49) and manually curated to remove artifacts using AliView (50). ML phylogenetic trees were estimated using IQ-TREE2 (51) under the General Time Reversible (GTR) nucleotide substitution model, which was

inferred as the best-fit model by the ModelFinder application implemented in IQ-TREE2 (*52*). Statistical support for tree nodes was estimated using a ML bootstrap approach with 1000 replicates. To investigate the temporal signal in our YFV datasets (datasets 1 to 3), we regressed root-to-tip genetic distances from this ML tree against sample collection dates using TempEst v.1.5.1 (*26*).

Dated phylogenetics
To estimate time-calibrated phylogenies, we conducted a phylogenetic analysis using a Bayesian approach (*53*). Accordingly, we used the GTR+gamma4 nucleotide substitution model and Bayesian Skyline tree prior as used previously (*18*) with an uncorrelated relaxed clock with a lognormal distribution (*18*). Analyses were run in duplicate in BEAST v.1.10.4 for 100 million MCMC steps, sampling parameters, and trees every 10,000th step. Convergence of MCMC chains was checked using Tracer (*54*). Maximum clade credibility (MCC) trees were summarized using TreeAnnotator after discarding 10% as burn-in.

Phylogeographic analyses
To model the phylogenetic diffusion of YFV SA1 lineages 1 and 2, we used a flexible relaxed random walk diffusion model (*55*, *56*) that accommodates branch-specific variation in rates of dispersal with a Cauchy distribution and a jitter window site of 0.01 (*57*, *58*). For each sequence, coordinates of latitude and longitude were attributed. MCMC analyses were performed in BEAST v1.10.4, running in duplicate for 100 million interactions and sampling every 10,000 steps in the chain. Convergence for each run was assessed in Tracer (effective sample size for all relevant model parameters, >200). MCC trees for each run were summarized using TreeAnnotator after discarding the initial 10% as burn-in. Last, we used the R package "seraphim" version 1.0 (*57*) to extract and map spatiotemporal information embedded in the posterior trees.

Eco-epidemiological data and integration with genomic data
Data of weekly notified and laboratory confirmed cases of infection by YFV in Brazil during 2015 to 2022 were supplied by the Brazilian Ministry of Health. A mosquito-viral suitability measure (index *P*) was estimated using the MVSE R-package v1.01 (*21*). The index *P* receives as input local temperature, humidity, and proposed probability distributions for key viral, vector, and host parameters related to the host-pathogen system under study. Accordingly, it measures the reproductive (transmission) potential of a single adult female mosquito in a completely susceptible host population. For parameterization, we used satellite climate data from Copernicus.eu (dataset "ERA5-Land monthly averaged data from 1950 to present"; https://cds.climate.copernicus.eu/), and parameter probability distributions informed by the literature. Because of lack of empirical data to calibrate index *P* specifically to mosquito species driving YFV transmission in the animal reservoir (e.g., Haemagogous and Sabethes spp.), the index was calibrated to *A. aegypti* and interpreted as a proxy for the risk of spillover to human populations. A full description of index *P* parameterization can be found in Supplementary Text. We used R v4.1.2 to calculate the correlation between incidence and index *P* using Spearman's rank correlation coefficient (function cor.test) and to determine best time lag between the two-time series (function ccf).

Bayesian modeling of YFV human case counts
We modeled human case counts and candidate covariates by municipality using the Besag York Mollié model (BYM2). Briefly, this model assumes a Poisson distribution for case counts and includes both spatial covariates and random effects to account for unexplained spatial variation. The model was implemented in R v4.1.2 and Stan. A full description of covariates, the model, and its output (posterior distributions) are provided in Supplementary Text.

Supplementary Materials
This PDF file includes:
S1 to S3
Tables S1 to S5
Figs. S1 to S6
References

REFERENCES AND NOTES
1. B. T. Lindenbach, C. L. Murray, H.-J. Thiel, C. Rice, Flaviviridae, in *Fields Virology*, D. M. Knipe, P. M. Howley, Eds. (Lippincott Williams & Wilkins, Philadelphia, 2013), pp. 712–746.
2. T. P. Monath, P. F. C. Vasconcelos, Yellow fever. *J. Clin. Virol.* **64**, 160–173 (2015).
3. N. I. O. Silva, L. Sacchetto, I. M. Rezende, G. D. S. Trindade, A. D. Labeaud, B. Thoisy, B. P. Drumond, Recent sylvatic yellow fever virus transmission in Brazil: The news from an old disease. *Virol. J.* **17**, 9 (2020).
4. P. F. C. Vasconcelos, J. E. Bryant, A. P. A. Travassos da Rosa, R. B. Tesh, S. G. Rodrigues, A. D. T. Barrett, Genetic divergence and dispersal of yellow fever virus, Brazil. *Emerg. Infect. Dis.* **10**, 1578–1584 (2004).
5. L. Sacchetto, B. P. Drumond, B. A. Han, M. L. Nogueira, N. Vasilakis, Re-emergence of yellow fever in the neotropics - quo vadis? *Emerg. Top. Life Sci.* **4**, 399–410 (2020).
6. P. F. Vasconcelos, S. G. Rodrigues, N. Degallier, M. A. Moraes, J. F. da Rosa, E. S. da Rosa, B. Mondet, V. L. Barros, A. P. da Rosa, An epidemic of sylvatic yellow fever in the southeast region of Maranhao State, Brazil, 1993–1994: Epidemiologic and entomologic findings. *Am. J. Trop. Med. Hyg.* **57**, 132–137 (1997).
7. N. R. Faria, M. U. G. Kraemer, S. C. Hill, J. Goes de Jesus, R. S. Aguiar, F. C. M. Iani, J. Xavier, J. Quick, L. Du Plessis, S. Dellicour, J. Thézé, R. D. O. Carvalho, G. Baele, C. H. Wu, P. P. Silveira, M. B. Arruda, M. A. Pereira, G. C. Pereira, J. Lourenço, U. Obolski, L. Abade, T. I. Vasylyeva, M. Giovanetti, D. Yi, D. J. Weiss, G. R. W. Wint, F. M. Shearer, S. Funk, B. Nikolay, V. Fonseca, T. E. R. Adelino, M. A. A. Oliveira, M. V. F. Silva, L. Sacchetto, P. O. Figueiredo, I. M. Rezende, E. M. Mello, R. F. C. Said, D. A. Santos, M. L. Ferraz, M. G. Brito, L. F. Santana, M. T. Menezes, R. M. Brindeiro, A. Tanuri, F. C. P. Dos Santos, M. S. Cunha, J. S. Nogueira, I. M. Rocco, A. C. da Costa, S. C. V. Komninakis, V. Azevedo, A. O. Chieppe, E. S. M. Araujo, M. C. L. Mendonça, C. C. dos Santos, C. D. dos Santos, A. M. Mares-Guia, R. M. R. Nogueira, P. C. Sequeira, R. G. Abreu, M. H. O. Garcia, A. L. Abreu, O. Okumoto, E. G. Kroon, C. F. C. de Albuquerque, K. Lewandowski, S. T. Pullan, M. Carroll, T. de Oliveira, E. C. Sabino, R. P. Souza, M. A. Suchard, P. Lemey, G. S. Trindade, B. P. Drumond, A. M. B. Filippis, N. J. Loman, S. Cauchemez, L. C. J. Alcantara, O. G. Pybus, Genomic and epidemiological monitoring of yellow fever virus transmission potential. *Science* **361**, 894–899 (2018). https://doi.org/10.1126/science.aat7115.
8. Brazilian Ministry of Health, Febre Amarela (2020); https://gov.br/saude/pt-br/assuntos/saude-de-a-a-z/f/febre-amarela-1.
9. M. A. B. de Almeida, E. Dos Santos, J. da Cruz Cardoso, D. Fernandes da Fonseca, C. A. Noll, V. R. Silveira, A. Y. Maeda, R. Pereira de Souza, C. Kanamura, R. A. Brasil, Yellow fever outbreak affecting Alouatta populations in southern Brazil (Rio Grande do Sul State), 2008-2009. *Am. J. Primatol.* **74**, 68–76 (2012).
10. A. P. M. Romano, Z. G. A. Costa, D. G. Ramos, M. A. Andrade, V. de Sá Jaime, M. A. B. de Almeida, K. C. Vettorello, M. Mascheretti, B. Flannery, Yellow fever outbreaks in unvaccinated populations, Brazil, 2008–2009. *PLOS Negl. Trop. Dis.* **8**, e2740 (2014).
11. M. Chame, L. Abdalla, A. Pinter, P. M. A. Romano, E. Krempser, G. Ramos, P. H. O. Passos, P. C. L. Silva, G. M. P. Silva, R. R. Gatti, D. A. Augusto, L. Sianto, Primates in SISS-Geo: Potential contributions of mobile technology, health surveillance and citizen science to support species conservation in Brazil. *Neotrop. Primates* **26**, 80–89 (2020).
12. Brazilian Ministry of Health, Situação epidemiológica da febre amarela no monitoramento 2019/2020. Brasília, Brazil (2020); https://gov.br/saude/pt-br/centrais-de-conteudo/publicacoes/boletins/boletins-epidemiologicos/edicoes/2020/boletim-epidemiologico-vol-51-no-01/@@download/file/boletim-epidemiologico-svs-01.pdf.
13. Brazilian Ministry of Health, Situação epidemiológica da febre amarela no monitoramento 2020/2021. Brasília, Brazil (2021/2022); https://gov.br/saude/pt-br/centrais-de-conteudo/publicacoes/boletins/boletins-epidemiologicos/edicoes/2021/boletim_epidemiologico_svs_31.pdf.

14. Minas Gerais State Department of Health, Febre Amarela (2022); https://saude.mg.gov.br/febreamarela.

15. M. S. Andrade, F. S. Campos, A. A. S. Campos, F. V. S. Abreu, F. L. Melo, A. D. P. Sevá, J. D. C. Cardoso, E. Dos Santos, L. C. Born, C. M. D. D. Silva, N. F. D. Müller, C. H. Oliveira, A. J. J. D. Silva, D. Simonini-Teixeira, S. Bernal-Valle, M. A. M. M. Mares-Guia, G. R. Albuquerque, A. P. M. Romano, A. C. Franco, B. M. Ribeiro, P. M. Roehe, M. A. B. Almeida, Real-time genomic surveillance during the 2021 re-emergence of the yellow fever virus in Rio Grande do Sul State, Brazil. *Viruses* **13**, 1976 (2021).

16. C. Possas, R. Lourenço-de-Oliveira, P. L. Tauil, F. P. Pinheiro, A. Pissinatti, R. V. da Cunha, M. Freire, R. M. Martins, A. Homma, Yellow fever outbreak in Brazil: The puzzle of rapid viral spread and challenges for immunisation. *Mem. Inst. Oswaldo Cruz* **3**, 113–222 (2018).

17. E. Delatorre, F. V. Santos De Abreu, I. P. Ribeiro, M. M. Gómez, A. A. Cunha Dos Santos, A. Ferreira-De-Brito, M. Sebastião Alberto Santos Neves, I. Bonelly, R. M. De Miranda, N. D. Furtado, L. M. S. Raphael, L. de Fátima Fernandes Da Silva, M. G. De Castro, D. G. Ramos, A. P. Martins Romano, E. G. Kallás, A. C. P. Vicente, G. Bello, R. Lourenço-De-Oliveira, M. C. Bonaldo, Distinct YFV lineages co-circulated in the central-western and Southeastern Brazilian regions from 2015 to 2018. *Front. Microbiol.* **10**, 1079 (2019).

18. M. Giovanetti, M. C. L. de Mendonça, V. Fonseca, M. A. Mares-Guia, A. Fabri, J. Xavier, J. G. de Jesus, T. Gräf, C. D. Dos Santos Rodrigues, C. C. Dos Santos, S. A. Sampaio, F. L. L. Chalhoub, F. de Bruycker Nogueira, J. Theze, A. P. M. Romano, D. G. Ramos, A. L. de Abreu, W. K. Oliveira, R. F. do Carmo Said, C. F. C. de Alburque, T. de Oliveira, C. A. Fernande, S. F. Aguiar, A. Chieppe, P. C. Sequeira, N. R. Faria, R. V. Cunha, L. C. J. Alcantara, A. M. B. de Filippis, Yellow fever virus reemergence and spread in Southeast Brazil, 2016–2019. *J. Virol.* **94**, e01623-19 (2019).

19. D. Couto-Lima, Y. Madec, M. I. Bersot, S. S. Campos, M. de Albuquerque Motta, F. Barreto dos Santos, M. Vazeille, P. F. da Costa Vasconcelos, R. Lourenço-de-Oliveira, A.-B. Failloux, Potential risk of re-emergence of urban transmission of Yellow Fever virus in Brazil facilitated by competent *Aedes* populations. *Sci. Rep.* **7**, 4848 (2017).

20. A. P. M. Romano, D. G. Ramos, F. A. A. Araújo, G. A. M. de Siqueira, M. P. D. Ribeiro, S. G. Leal, A. N. M. S. Elkhoury, Febre amarela no Brasil: Recomendações para a vigilância, prevenção e controle. *Epidemiol. Serv. Saúde* **20**, 101–106 (2011).

21. U. Obolski, P. N. Perez, C. J. Villabona-Arenas, J. Thézé, N. R. Faria, J. Lourenço, MVSE: An R-package that estimates a climate-driven mosquito-borne viral suitability index. *Methods Ecol. Evol.* **10**, 1357–1370 (2019).

22. T. Nakase, M. Giovanetti, U. Obolski, J. Lourenço, Global transmission suitability maps for dengue virus transmitted by *Aedes aegypti* from 1981 to 2019. *Sci Data* **10**, 275 (2023).

23. S. H. Tuboi, Z. G. Costa, P. F. da Costa Vasconcelos, D. Hatch, Clinical and epidemiological characteristics of yellow fever in Brazil: Analysis of reported cases 1998-2002. *Trans. R. Soc. Trop. Med. Hyg.* **101**, 169–175 (2007).

24. R. B. Kaul, M. V. Evans, C. C. Murdock, J. M. Drake, Spatio-temporal spillover risk of yellow fever in Brazil. *Parasit. Vectors* **11**, 488 (2018).

25. M. P. Cunha, A. N. Duarte-Neto, S. Z. Pour, A. S. Ortiz-Baez, J. C. Cerný, B. B. S. Pereira, C. T. Braconi, Y.-L. Ho, B. Perondi, J. Sztajnbok, V. A. F. Alves, M. Dolhnikoff, E. C. Holmes, P. H. N. Saldiva, P. M. A. Zanotto, Origin of the São Paulo Yellow Fever epidemic of 2017–2018 revealed through molecular epidemiological analysis of fatal cases. *Sci. Rep.* **9**, 20418–20418 (2019).

26. A. Rambaut, T. T. Lam, L. Max Carvalho, O. G. Pybus, Exploring the temporal structure of heterochronous sequences using TempEst (formerly Path-O-Gen). *Virus Evol.* **2**, vew007 (2016).

27. P. F. C. Vasconcelos, A. F. Sperb, H. A. O. Monteiro, M. A. N. Torres, M. R. S. Sousa, H. B. Vasconcelos, L. B. Mardini, S. G. Rodrigues, Isolations of yellow fever virus from *Haemagogus leucocelaenus* in Rio Grande do Sul State, Brazil. *Trans. R. Soc. Trop. Med. Hyg.* **97**, 60–62 (2003).

28. J. C. Cardoso, M. A. B. Almeida, E. Santos, D. F. Fonseca, M. A. M. Sallum, C. A. Noll, H. A. de Oliveira Monteiro, A. C. R. Cruz, V. L. Carvalho, E. V. Pinto, F. C. Castro, J. P. Nunes Neto, M. N. O. Segura, P. F. C. Vasconcelos, Yellow fever virus in *Haemagogus leucocelaenus* and *Aedes serratus* mosquitoes, Southern Brazil, 2008. *Emerg. Infect. Dis.* **16**, 1918–1924 (2010).

29. M. S. Andrade, F. S. Campos, C. H. Oliveira, R. S. Oliveira, A. A. S. Campos, M. A. B. Almeida, V. S. Fonseca, D. Simonini-Teixeira, A. P. Sevá, A. O. D. Temponi, F. M. Magalhães, D. C. C. Chaves, M. A. Pereira, L. O. Lamounier, G. G. Menezes, S. M. Aquino-Teixeira, M. A. Gonçalves-dos-Santos, S. B. Valle, N. F. D. Müller, J. C. Cardoso, E. Santos, M. Mares-Guia, G. R. Albuquerque, A. P. M. Romano, A. C. Franco, B. M. Ribeiro, P. M. Roehe, F. Abreu, Fast surveillance response reveals the introduction of a new Yellow Fever Virus sub-lineage in 2021, in Minas Gerais, Brazil. *Mem. Inst. Oswaldo Cruz* **117**, e220127 (2022).

30. J. A. Marengo, T. Ambrizzi, L. M. Alves, N. J. C. Barreto, M. Simões Reboita, A. M. Ramos, Changing Trends in Rainfall Extremes in the Metropolitan Area of São Paulo: Causes and Impacts. *Front. Clim.* **3**, 45–89 (2020).

31. P. Regoto, C. Dereczynski, S. C. Chou, A. C. Bazzanela, Observed changes in air temperature and precipitation extremes over Brazil. *Int. J. Climatol.* **41**, 5125–5142 (2021).

32. A. P. Dobson, S. L. Pimm, L. Hannah, L. Kaufman, J. A. Ahumada, A. W. Ando, A. Bernstein, J. Busch, P. Daszak, J. Engelmann, M. F. Kinnaird, B. V. Li, T. Loch-Temzelides, T. Lovejoy, K. Nowak, P. R. Roehrdanz, M. M. Vale, Ecology and economics for pandemic prevention. *Science* **369**, 379–381 (2020).

33. S. P. Ribeiro, M. M. Vale, J. A. F. Diniz-Filho, G. W. Fernandes, A. B. Reis, C. E. V. Grelle, Heading back into the perfect storm: Increasing risks for disease emergence in Brazil? *J. Braz. Soc. Trop. Med.* **55**, 6–40 (2021).

34. Global Forest Watch, Monitoramento de Florestas Projetado para a Ação, *Forest Monitoring Designed for Action* (2022); https://globalforestwatch.org/map/.

35. J. I. Rosser, K. Nielsen-Saines, E. Saad, T. Fuller, Reemergence of yellow fever virus in southeastern Brazil, 2017-2018: What sparked the spread? *PLOS Negl. Trop. Dis.* **16**, e0010133 (2022).

36. National Institute of Spatial Research, Programa Queimadas. Monitoramento dos focos Ativos por Estado, *Burn Program. Monitoring of Active Fires by State* (2022); https://queimadas.dgi.inpe.br/queimadas/portal-static/estatisticas_estados/.

37. E. S. Brondízio, A. Cak, M. Caldas, C. F. Memna, R. E. Bilsborrow, C. Futemma, T. Ludwigs, E. Moran, M. Batistella, Small farmers and deforestation in amazônia. *Geophys. Monogr. Ser.* **186**, 117–143 (2009).

38. C. Schneider, E. Coudel, F. Cammelli, P. Sablayrolles, Small-scale farmers' needs to end deforestation: Insights for REDD+ in São Felix do Xingu (Pará, Brazil). *Int. For. Rev.* **17**, 124–142 (2015).

39. E. S. Moreno, I. Agostini, I. Holzmann, M. S. D. Bitetti, L. I. Oklander, M. M. Kowalewski, P. M. Beldomenico, S. Goenaga, M. Martínez, E. Lestani, A. L. J. Desbiez, P. Miler, Yellow fever impact on brown howler Monkeys (*Alouatta guariba clamitans*) in Argentina: A meta-modelling approach based on population viability analysis and epidemiological dynamics. *Mem. Inst. Oswaldo Cruz* **110**, 865–876 (2015).

40. B. de Thoisy, N. I. O. Silva, L. Sacchetto, G. de Souza Trindade, B. P. Drumond, Spatial epidemiology of yellow fever: Identification of determinants of the 2016-2018 epidemics and at-risk areas in Brazil. *PLOS Negl. Trop. Dis.* **14**, e0008691 (2020).

41. T. R. Tisler, F. Z. Teixeira, R. A. A. Nóbrega, Conservation opportunities and challenges in Brazil's roadless and railroad-less areas. *Sci. Adv.* **8**, 8–48 (2022).

42. S. L. Li, A. L. Acosta, S. C. Hill, O. J. Brady, M. A. B. de Almeida, J. D. C. Cardoso, A. Hamlet, L. F. Mucci, J. Telles de Deus, F. C. M. Iani, N. S. Alexander, G. R. W. Wint, O. G. Pybus, M. U. G. Kraemer, N. R. Faria, J. P. Messina, Mapping environmental suitability of *Haemagogus* and *Sabethes* spp. mosquitoes to understand sylvatic transmission risk of yellow fever virus in Brazil. *PLoS Negl. Trop. Dis.* **16**, e0010019 (2022).

43. IUCN, The IUCN Red List of Threatened Species. Version 2022-1 (2022); https://iucnredlist.org.

44. J. M. Dietz, S. J. Hankerson, B. R. Alexandre, M. D. Henry, A. F. Martins, L. P. Ferraz, C. R. Ruiz-Miranda, Yellow fever in Brazil threatens successful recovery of endangered golden lion tamarins. *Sci. Rep.* **9**, 12926 (2019).

45. T. É. R. Adelino, M. Giovanetti, V. Fonseca, J. Xavier, Á. S. de Abreu, V. A. do Nascimento, L. H. F. Demarchi, M. A. A. Oliveira, V. L. da Silva, A. L. E. S. de Mello, G. M. Cunha, R. H. Santos, E. C. de Oliveira, J. A. C. Júnior, F. C. de Melo Iani, A. M. B. de Filippis, A. L. de Abreu, R. de Jesus, C. F. C. de Albuquerque, J. M. Rico, R. F. do Carmo Said, J. A. Silva, N. F. O. de Moura, P. Leite, L. C. V. Frutuoso, S. K. Haddad, A. Martínez, F. K. Barreto, C. C. Vazquez, R. V. da Cunha, E. L. L. Araújo, S. F. de Oliveira Tosta, A. de Araújo Fabri, F. L. L. Chalhoub, P. da Silva Lemos, F. de Bruycker-Nogueira, G. G. de Castro Lichs, M. C. S. U. Zardin, F. M. C. Segovia, C. C. M. Gonçalves, Z. D. C. F. Grillo, S. N. Slavov, L. A. Pereira, A. F. Mendonça, F. M. Pereira, J. J. F. de Magalhães, A. C. M. dos Santos Júnior, M. M. de Lima, R. M. R. Nogueira, A. Góes-Neto, V. A. de Carvalho Azevedo, D. B. Ramalho, W. K. Oliveira, E. M. Macario, A. C. de Medeiros, V. Pimentel; Latin American Genomic Surveillance Arboviral Network, E. C. Holmes, E. de Oliveira, J. Lourenço, L. C. J. Alcantara, Field and classroom initiatives for portable sequence-based monitoring of dengue virus in Brazil. *Nat. Commun.* **12**, 229 (2021).

46. C. Domingo, P. Patel, J. Yillah, M. Weidmann, J. A. Méndez, E. R. Nakouné, M. Niedrig, Advanced yellow fever virus genome detection in point-of-care facilities and reference laboratories. *J. Clin. Microbiol.* **50**, 4054–4060 (2012).

47. J. Quick, N. D. Grubaugh, S. T. Pullan, I. M. Claro, A. D. Smith, K. Gangavarapu, G. Oliveira, R. Robles-Sikisaka, T. F. Rogers, N. A. Beutler, D. R. Burton, L. L. Lewis-Ximenez, J. G. de Jesus, M. Giovanetti, S. C. Hill, A. Black, T. Bedford, M. W. Carroll, M. Nunes, L. C. Alcantara Jr., E. C. Sabino, S. A. Baylis, N. R. Faria, M. Loose, J. T. Simpson, O. G. Pybus, K. G. Andersen, N. J. Loman, Multiplex PCR method for MinION and Illumina sequencing of Zika and other virus genomes directly from clinical samples. *Nat. Protoc.* **12**, 1261–1276 (2017).

48. M. Vilsker, Y. Moosa, S. Nooij, V. Fonseca, Y. Ghysens, K. Dumon, R. Pauwels, L. C. Alcantara, E. V. Eynden, A.-M. Vandamme, K. Deforche, T. de Oliveira, Genome detective: An automated system for virus identification from high-throughput sequencing data. *Bioinformatics* **35**, 871–873 (2019).

49. K. Katoh, D. M. Standley, MAFFT Multiple Sequence Alignment Software Version 7: Improvements in performance and usability. *Mol. Biol. Evol.* **30**, 772–780 (2013).

50. A. Laarson, AliView: A fast and lightweight alignment viewer and editor for large datasets. *Bioinformatics* **30**, 3276–3278 (2014).

51. L. T. Nguyen, H. A. Schmidt, A. von Haeseler, B. Q. Minh, IQ-TREE: A fast and effective stochastic algorithm for estimating maximum-likelihood phylogenies. *Mol. Biol. Evol.* **32**, 268–274 (2015).

52. S. Kalyaanamoorthy, B. Q. Minh, T. K. F. Wong, A. von Haeseler, L. S. Jermiin, ModelFinder: Fast model selection for accurate phylogenetic estimates. *Nat. Methods* **14**, 587–589 (2017).

53. M. A. Suchard, P. Lemey, G. Baele, D. L. Ayres, A. J. Drummond, A. Rambaut, Bayesian phylogenetic and phylodynamic data integration using BEAST 1.10. *Virus Evol.* **4**, vey016 (2018).

54. A. Rambaut, A. J. Drummond, D. Xie, G. Baele, M. A. Suchard, Posterior summarization in Bayesian phylogenetics using Tracer 1.7. *Syst. Biol.* **67**, 901–904 (2018).

55. P. Lemey, A. Rambaut, J. J. Welch, M. A. Suchard, Phylogeography takes a relaxed random walk in continuous space and time. *Mol. Biol. Evol.* **27**, 1877–1885 (2010).

56. O. G. Pybus, M. A. Suchard, P. Lemey, F. J. Bernardin, A. Rambaut, F. W. Crawford, R. R. Gray, N. Arinaminpathy, S. L. Stramer, M. P. Busch, E. L. Delwart, Unifying the spatial epidemiology and molecular evolution of emerging epidemics. *Proc. Natl. Acad. Sci. U.S.A.* **109**, 15066–15071 (2012).

57. S. Dellicour, R. Rose, N. R. Faria, P. Lemey, O. G. Pybus, SERAPHIM: Studying environmental rasters and phylogenetically informed movements. *Bioinformatics* **32**, 3204–3206 (2016).

58. S. Dellicour, M. S. Gill, N. R. Faria, A. Rambaut, Relax, keep walking - a practical guide to continuous phylogeographic inference with BEAST. *Mol. Biol. Evol.* **38**, 3486–3493 (2021).

59. J. Lourenço, M. M. de Lima, N. R. Faria, A. Walker, M. U. G. Kraemer, C. J. Villabona-Arenas, B. Lambert, E. M. de Cerqueira, O. G. Pybus, L. C. Alcantara Jr., M. Recker, Epidemiological and ecological determinants of Zika virus transmission in an urban setting. *eLife* **6**, e29820 (2017).

60. M. E. Petrone, R. Earnest, J. Lourenço, M. U. G. Kraemer, R. Paulino-Ramirez, N. D. Grubaugh, L. Tapia, Asynchronicity of endemic and emerging mosquito-borne disease outbreaks in the Dominican Republic. *Nat. Commun.* **12**, 151 (2021).

61. J. Lourenço, F. Pinotti, T. Nakase, M. Giovanetti, U. Obolski, Letter to the editor: Atypical weather is associated with the 2022 early start of West Nile virus transmission in Italy. *Euro Surveill.* **27**, 90–990 (2022).

62. J. Lourenço, S. C. Barros, L. Zé-Zé, D. S. C. Damineli, M. Giovanetti, H. C. Osório, F. Amaro, A. M. Henriques, F. Ramos, T. Luís, M. D. Duarte, T. Fagulha, M. J. Alves, U. Obolski, West Nile virus transmission potential in Portugal. *Commun. Biol.* **5**, 6 (2022).

63. J. Lourenço, R. N. Thompson, J. Thézé, U. Obolski, Characterising West Nile virus epidemiology in Israel using a transmission suitability index. *Eurosurveillance* **25**, 190–629 (2020).

64. L. E. Hugo, J. A. L. Jeffery, B. J. Trewin, L. F. Wockner, N. T. Yen, N. H. Le, L. E. Nghia, E. Hine, P. A. Ryan, B. H. Kay, Adult survivorship of the dengue mosquito *Aedes aegypti* varies seasonally in central Vietnam. *PLOS Negl. Trop. Dis.* **8**, 26–69 (2014).

65. M. Trpis, W. Häusermann, G. B. Craig Jr., Estimates of population size, dispersal, and longevity of domestic *Aedes aegypti* (Diptera: Culicidae) by mark-release-recapture in the village of Shauri Moyo in eastern Kenya. *J. Med. Entomol.* **32**, 27–33 (1995).

66. M. Trpis, W. Hausermann, Dispersal and other population parameters of *Aedes aegypti* in an African village and their possible significance in epidemiology of vector-borne diseases. *Am. J. Trop. Med. Hyg.* **35**, 1263–1279 (1986).

67. M. A. Johansson, N. Arana-Vizcarrondo, J. Erin Staples, Incubation periods of yellow fever virus. *Am. J. Trop. Med. Hyg.* **83**, 183–188 (2010).

68. E. Hindle, The transmission of yellow fever. *Lancet* **216**, 835–842 (1930).

69. H. Beeuwkes, Clinical manifestations of yellow fever in the West African native as observed during four extensive epidemics of the disease in the Gold Coast and Nigeria∗. *Trans. R. Soc. Trop. Med. Hyg.* **30**, 61–86 (1936).

70. N. P. Hudson, C. B. Philip, Infectivity of blood during the course of experimental yellow fever. *J. Exp. Med.* **50**, 583–599 (1929).

71. R. Tacutu, D. Thornton, E. Johnson, A. Budovsky, D. Barardo, T. Craig, E. Diana, G. Lehmann, D. Toren, J. Wang, V. E. Fraifeld, J. P. de Magalhães, Human Ageing Genomic Resources: New and updated databases. *Nucleic Acids Res.* **46**, D1083–D1090 (2018).

72. M. Morris, Spatial Models in Stan: Intrinsic Auto-Regressive Models for Areal Data; https://mc-stan.org/users/documentation/case-studies/icar_stan.html.

73. J. Besag, J. York, A. Mollié, Bayesian image restoration, with two applications in spatial statistics. *Ann. Inst. Stat. Math.* **43**, 1–20 (1991).

74. A. Riebler, S. H. Sørbye, D. Simpson, H. Rue, An intuitive Bayesian spatial model for disease mapping that accounts for scaling. *Stat. Methods Med. Res.* **25**, 1145–1165 (2016).

75. F. M. Shearer, C. L. Moyes, D. M. Pigott, O. J. Brady, F. Marinho, A. Deshpande, J. Longbottom, A. J. Browne, M. U. G. Kraemer, K. M. O'Reilly, J. Hombach, S. Yactayo, V. E. M. de Araújo, A. A. da Nóbrega, J. F. Mosser, J. D. Stanaway, S. S. Lim, S. I. Hay, N. Golding, R. C. Reiner Jr.,

76. M. Buchhorn, B. Smets, L. Bertels, B. De Roo, M. Lesiv, N. E. Tsendbazar, L. Li, A. Tarko, Copernicus Global Land Service: Land Cover 100m: Version 3 Globe 2015-2019: Product User Manual, Zenodo, Geneve, Switzerland, September 2020, pp. 34–90.

Global yellow fever vaccination coverage from 1970 to 2016: An adjusted retrospective analysis. *Lancet Infect. Dis.* **17**, 1209–1217 (2017).

77. L. Abdalla, D. A. Augusto, M. Chame, A. S. Dufek, L. Oliveira, E. Krempser, Statistically enriched geospatial datasets of Brazilian municipalities for data-driven modeling. *Sci Data* **9**, 34–489 (2022).

78. K. Jordahl, J. Van den Bossche, M. Fleischmann, J. Wasserman, J. McBride, J. Gerard, J. Tratner, M. Perry, A. G. Badaracco, C. Farmer, G. A. Hjelle, A. D. Snow, M. Cochran, S. Gillies, L. Culbertson, M. Bartos, N. Eubank, maxalbert, A. Bilogur, S. Rey, C. Ren, D. Arribas-Bel, L. Wasser, L. J. Wolf, M. Journois, J. Wilson, A. Greenhall, C. Holdgraf, Filipe, F. Leblanc, geopandas/geopandas: v0.8.1. 2020; https://zenodo.org/record/3946761.

79. Stan, in stan-dev.github.io [Internet] (2022); https://mc-stan.org.

80. RStan: The R interface to Stan. Website, in Stan Development Team. R package version 2.21.7 (2022); https://mc-stan.org/.

81. P. A. P. Moran, Notes on continuous stochastic phenomena. *Biometrika* **37**, 17–23 (1950).

Science Advances

Genomic epidemiology unveils the dynamics and spatial corridor behind the Yellow Fever virus outbreak in Southern Brazil

Marta Giovanetti, Francesco Pinotti, Camila Zanluca, Vagner Fonseca, Taishi Nakase, Andrea C. Koishi, Marcel Tscha, Guilherme Soares, Gisiane Gruber Dorl, Antônio Ernesto M.L Marques, Renato Sousa, Talita Emile Ribeiro Adelino, Joilson Xavier, Carla de Oliveira, Sandro Patroca, Natalia Rocha Guimaraes, Hegger Fritsch, Maria Angélica Mares-Guia, Flavia Levy, Pedro Henrique Passos, Vinicius Leme da Silva, Luiz Augusto Pereira, Ana Flávia Mendonça, Isabel Luana de Macêdo, Davi Emanuel Ribeiro de Sousa, Gabriela Rodrigues de Toledo Costa, Marcio Botelho de Castro, Miguel de Souza Andrade, Filipe Vieira Santos de Abreu, Fabrício Souza Campos, Felipe Campos de Melo Iani, Maira Alves Pereira, Karina Ribeiro Leite Jardim Cavalcante, Andre Ricardo Ribas de Freitas, Carlos Frederico Campelo de Albuquerque, Eduardo Marques Macário, Marlei Pickler Debiasi dos Anjos, Rosane Campanher Ramos, Aline Alves Scarpellini Campos, Adriano Pinter, Marcia Chame, Livia Abdalla, Irina Nastassja Riediger, Sérvio Pontes Ribeiro, Ana I. Bento, Tulio de Oliveira, Carla Freitas, Noely Fabiana Oliveira de Moura, Allison Fabri, Cintia Damasceno dos Santos Rodrigues, Carolina Cardoso Dos Santos, Marco Antonio Barreto de Almeida, Edmilson dos Santos, Jader Cardoso, Douglas Adriano Augusto, Eduardo Krempser, Luís Filipe Mucci, Renata Rispoli Gatti, Sabrina Fernandes Cardoso, João Augusto Brancher Fuck, Maria Goretti David Lopes, Ivana Lucia Belmonte, Gabriela Mayoral Pedroso da Silva, Maiane Regina Ferreira Soares, Marilia de Melo Santos de Castilhos, Joseana Cardoso de Souza e Silva, Alceu Bisetto Junior, Emanuelle Gemin Pouzato, Laurina Setsuko Tanabe, Daniele Akemi Arita, Ricardo Matsuo, Josiane dos Santos Raymundo, Paula Cristina Linder Silva, Ana Santana Araújo Ferreira Silva, Sandra Samila, Glauco Carvalho, Rodrigo Stabeli, Wildo Navegantes, Luciano Andrade Moreira, Alvaro Gil A. Ferreira, Guilherme Garcia Pinheiro, Bruno Tardelli Diniz Nunes, Daniele Barbosa de Almeida Medeiros, Ana Cecília Ribeiro Cruz, Rivaldo Venâncio da Cunha, Wes Van Voorhis, Ana Maria Bispo de Filippis, Maria Almiron, Edward C. Holmes, Daniel Garkauskas Ramos, Alessandro Romano, José Lourenço, Luiz Carlos Junior Alcantara, and Claudia Nunes Duarte dos Santos

View the article online
https://www.science.org/doi/10.1126/sciadv.adg9204
Permissions
https://www.science.org/help/reprints-and-permissions

Use of this article is subject to the Terms of service